Importance of Residue 13 and the C-Terminus for the Structure and Activity of the Antimicrobial Peptide Aurein 2.2

John T. J. Cheng,[†] John D. Hale,[‡] Jason Kindrachuk,[‡] Havard Jessen,[‡] Melissa Elliott,[‡] Robert E. W. Hancock,[‡] and Suzana K. Straus[†*]

[†]Department of Chemistry and [‡]Centre for Microbial Diseases and Immunity Research, University of British Columbia, Vancouver, British Columbia, Canada

ABSTRACT Previous studies on aurein 2.2 and 2.3 in DMPC/DMPG and POPC/POPG membranes have shown that bilayer thickness and phosphatidylglycerol content have a significant impact on the interaction of these peptides with membrane bilayers. Further examination with the $DiSC_35$ assay has indicated that aurein 2.2 induces greater membrane leakage than aurein 2.3 in *Staphylococcus aureus* C622. The only difference between these peptides is a Leu to Ile mutation at residue 13. To better understand the importance of this residue, the structure and activity of the L13A, L13F, and L13V mutants were investigated. In addition, we investigated a number of peptides with truncations at the C-terminus to determine whether the C-terminus, which contains residue 13, is crucial for antimicrobial activity. Solution circular dichroism results demonstrated that the L13F mutation and the truncation of the C-terminus by six residues resulted in decreased helical content, whereas the L13A or L13V mutation and the truncation of the C-terminus by three residues showed little to no effect on the structure. Oriented circular dichroism results demonstrated that only an extensive C-terminal truncation reduced the ability of the peptide to insert into lipid bilayers. ^{31}P NMR spectroscopy showed that all peptides disorder the headgroups. The implications of these results in terms of antimicrobial activity and the ability of these peptides to induce leakage in *S. aureus* are discussed. The results suggest that the presence of the 13th residue in aurein 2.2 is important for structure and activity, but the exact nature of residue 13 is less important as long as it is a hydrophobic residue.

INTRODUCTION

Cationic antimicrobial peptides are an important class of peptides that are ubiquitous in nature and form an important part of the immune defense system of many plants and animals. Their unique property of displaying little or no intrinsic or mutational resistance (1–3) has led to wide interest in exploring them as alternatives to currently used antibiotics. Examples include a range of cationic antimicrobial peptides secreted by amphibians as part of their host-defense mechanisms (4,5). When these animals are exposed to various stresses or stimuli, they secrete a wide range of host-defense compounds, including amines, alkaloids, and peptides (4). Many studies have reviewed (4–6) or extensively characterized these peptides, including magainin (7–16), maculatin (17–22), and brevinins (23–28), and others, such as citropin 1.1 and aurein 1.2, from the Australian tree frogs *Litoria citropa* and *Litoria aurea* (17–20,22,29–31), respectively. The latter peptide is part of a larger family of peptides known as the aurein peptides, which range in length from 13 to 25 residues. Many aurein peptides carry an amidated C-terminus and exhibit broad-spectrum antimicrobial activity against Gram-positive bacteria and other disease-causing agents, such as cancerous cells (30).

Previous works examined the structure-function relationships of two members of the aurein peptide family, aurein 2.2 (GLFDIVKKVVGA**L**GSL-$CONH_2$) and aurein 2.3 (GLFDIVKKVVGA**I**GSL-$CONH_2$), as well as an inactive version of aurein 2.3 with a carboxy C-terminus (aurein 2.3-COOH) (32,33). Results from solution circular dichroism (CD) and oriented CD (OCD), solid-state ^{31}P NMR, calcein release assays, and differential scanning calorimetry experiments using DMPC/DMPG and POPC/POPG membranes demonstrated that the bilayer thickness and phosphatidylglycerol content have a significant impact on the behavior of these aurein peptides in different membrane environments (33). The model that emerged from these studies is that all three peptides cause significant membrane perturbations in DMPC/DMPG, leading to the formation of micelles. In POPC/POPG, on the other hand, all three peptides form (disordered) toroidal pores, with little leakage. Some of the data indicate that the observed membrane perturbation is dependent on the amino acid sequence. For instance, peptide-membrane interactions are concentration-dependent and differ among aurein 2.2, aurein 2.3, and aurein 2.3-COOH. Results from 3,3′-dipropylthiadicarbocyanine iodide ($DiSC_35$) assays, which measure the ability of peptides to dissipate the membrane potential gradient, have indicated that aurein 2.2 induces greater membrane leakage than aurein 2.3 in intact *Staphylococcus aureus* C622 cells. Given that aurein 2.2 and 2.3 have similar minimal inhibitory concentrations (MICs) (32), the difference in the ability of the peptide to perturb membranes indicates that aurein 2.2 and 2.3 may kill Gram-positive bacteria via somewhat different mechanisms.

Submitted June 11, 2010, and accepted for publication August 30, 2010.

*Correspondence: sstraus@chem.ubc.ca

Editor: Marc Baldus.

0006-3495/10/11/2926/10 $2.00

doi: 10.1016/j.bpj.2010.08.077

To elucidate the mechanism of action of aurein 2.2 and aurein 2.3, and to better understand how a subtle difference in sequence at residue 13 might affect the mode of action, we investigated peptides with mutations at position 13 and peptides with C-terminal truncations. Although a large number of peptides would be needed for a complete and comprehensive study, we were able to use prior information about the effect of mutations on other peptides (34–38) and limit our focus to five peptides. The first three peptides consisted of a single conservative mutation at residue 13 from one hydrophobic residue (L) to another. The peptides with L13A, L13F, and L13V were chosen specifically to probe the effect of steric hindrance (L13A mutation), aromatic ring-lipid interaction (L13F mutation), and hydrophobicity (L13V mutation) on structure and activity. The last two peptides consisted of the native aurein 2.2 sequence, with the last three (aurein 2.2-Δ3) or six residues missing (aurein 2.2-Δ6). In aurein 2.2-Δ3, residue 13 became the last residue in sequence, and in aurein 2.2-Δ6, residue 13 was completely removed. Since most of the peptides in the aurein family have conserved N-termini, we anticipated that a modest C-terminal truncation would have little effect on activity.

To determine the mode of action of the five peptides mentioned above, we determined their structure and activities. Solution CD spectroscopy was used to examine whether these peptides have different α-helical content in the membrane environment. To assess how these mutants interact with the lipid bilayers, we used OCD and ^{31}P NMR spectroscopy. $DiSC_3$5 assays (using *S. aureus* C622) were performed to examine whether changes in sequence affect the ability of peptides to disrupt intact cell bacterial membranes. Finally, the MIC of each peptide was determined against *S. aureus* strain C622 and *Staphylococcus epidermidis* strain C621 to correlate observations made in model membranes to the behavior of these aurein peptides in the presence of intact bacteria. Overall, these data allowed us to determine the role of specific residues in structure and activity, and to better understand how sequence variation modulates structure-function relationships.

MATERIALS AND METHODS

Materials

Details pertaining to the materials used in this study can be found in the Supporting Material.

Methods

Peptide synthesis and purification

Aurein 2.2 mutants (Table S1) were synthesized as previously described (32) using a peptide synthesizer (CS Bio Co., Menlo Park, CA) and in situ neutralization Fmoc chemistry. All peptides were C-terminally amidated. The crude peptide product was purified by preparative reverse-phase high-performance liquid chromatography on a Waters 600 system (Waters Limited, Mississauga, Ontario, Canada) as previously described (32,33). The identity of the products was verified and confirmed to be $\geq$99% pure. The molecular weights of the five aurein mutant peptides in this study (as well as aurein 2.3) can be found in Table S1.

Circular dichroism

Solution and oriented CD experiments were carried out using a J-810 spectropolarimeter (JASCO, Victoria, British Columbia, Canada) at 30°C as previously described (32) (see Supporting Material for sample preparation and further details).

NMR spectroscopy

Solid-state ^{31}P NMR experiments on mechanically aligned lipid bilayer samples were carried out on a Bruker 500-MHz NMR spectrometer (Milton, Ontario, Canada) at 30°C, operating at a phosphorus frequency of 202.40 MHz as previously reported (32). The 90° pulse was set to 11.25 μs (POPC/POPG) and a 3 s recycle delay was used. The spectra were acquired using 2048 scans and processed with 50 Hz line-broadening.

MIC determination

The MICs for L13A, L13F, L13V, aurein 2.2-Δ3, and aurein 2.2-Δ6 were determined based on a previously described methodology with modifications (39) (see the Supporting Material for more details).

$DiSC_3$5 assay

The ability of the aurein peptides to depolarize the cytoplasmic membrane of *S. aureus* C622 was determined using the membrane potential-sensitive dye 3,3′- dipropylthiadicarbocyanine iodide ($DiSC_3$5). C622 was grown to mid-logarithmic phase in LB media, centrifuged, washed in 5 mM HEPES and 20 mM glucose, and then resuspended in the same buffer to a final OD_{600} of 0.05. A final concentration of 200 mM KCl was added to the cells and left for 30 min at room temperature to equilibrate cytoplasmic and external K^+ concentrations before the $DiSC_3$5 was added at a final concentration of 0.8 μM for 30 min (see the Supporting Material for more details).

RESULTS

Secondary structure of the aurein mutants

Our previous studies (33) suggested that 1:1 POPC/POPG (mol/mol) membranes might be the most representative model for investigating the interaction of aurein peptides with Gram-positive bacteria. As presented in a recently submitted manuscript (J. T. J. Cheng, J. D. Hale, J. Kindrachuk, H. Jessen, M. Elliott, R. E. W. Hancock, and S. K. Straus), we explored this further by investigating the structure and membrane interaction of the five mutants studied here in 1:1 POPE/POPG (mol/mol) membranes and 1:1 cardiolipin/POPG (mol/mol) membranes. We found that both POPC/POPG and cardiolipin/POPG are good models for Gram-positive bacteria like *S. aureus* and *S. epidermidis*. Since these are the bacteria of interest in this study, we will therefore focus exclusively on the results obtained in 1:1 POPC/POPG.

The solution CD spectra of the five aurein mutants in 1:1 POPC/POPG (mol/mol) small unilamellar vesicles (SUVs) were recorded (Fig. S1). All spectra demonstrated a maximum at 190 nm and two minima at 207 nm and 222 nm, which are characteristic of α-helical structure.

This demonstrated that all five aurein mutants adopted an α-helical conformation in POPC/POPG SUVs. As previously observed (32), similar intensities were found for all peptide/lipid molar ratios (P/L = 1:15, 1:50, and 1:100) studied, indicating that maximum binding of the peptide to the lipid vesicles occurred (20). The CD data were then fitted using three different programs (CDSSTR (41), CONTINLL (42), and SELCON3 (43–45)) to determine secondary structure content under all conditions probed here. Fig. 1 shows the percentage of α-helical and random coil content as a function of P/L ratios for the five aurein mutants. The results show that all five aurein mutants adopted a close to 100% α-helical conformation at high P/L ratios. As previously observed (33), helical content increased with increasing peptide concentrations, indicating that high concentrations are needed to achieve maximum folding. At lower peptide concentrations, however, differences in helical content were observed. At a 1:50 P/L ratio, L13A, L13V, and aurein 2.2-Δ3 showed higher helical content (96 ~ 98%), whereas L13F and aurein 2.2-Δ6 showed lower helical content (53 ~ 66%). Overall, the data show that the structures of the five aurein mutants were retained but the structural content was dependent on the molar concentrations examined, and differences were significant at lower peptide concentrations.

Membrane insertion states of the mutant aurein peptides

Understanding the interaction of aurein mutants with model membranes is crucial for elucidating the effect of peptide modification on the extent of peptide insertion into the lipid bilayers. We conducted OCD experiments to investigate the peptide insertion profiles in 1:1 POPC/POPG (mol/mol) bilayers. For both OCD and solid-state ^{31}P NMR (see following section), the samples were prepared in a similar fashion so that the data sets could be directly compared and also to verify that the samples were aligned. All experiments were conducted at 30°C (liquid crystalline phase) for consistent comparison with our previous study. In addition, experiments were repeated at least twice to ensure reproducibility of the results.

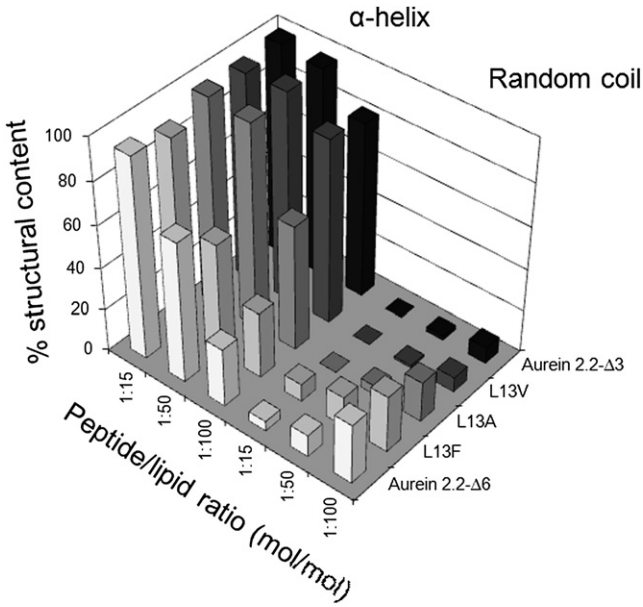

FIGURE 1 Secondary structure content of the five aurein mutants in 1:1 POPC/POPG (mol/mol) SUVs: the percentage of α-helical content and random coil content were plotted as a function of P/L ratios and aurein mutants (as indicated).

Fig. 2 shows OCD results for the aurein mutants in 1:1 POPC/POPG (mol/mol) bilayers as a function of P/L ratios. The spectra were normalized such that the intensities of all the spectra at 222 nm are the same. The spectra (Fig. 2, *b–d*) show that L13F, L13V, and aurein 2.2-Δ3 mutants inserted (inserted (I-state) or tilt (T-state)) into POPC/POPG bilayers at threshold P/L molar ratios between 1:80 and 1:120, and were surface adsorbed (S-state) at P/L ratios > 1:120 (mol/mol). L13A showed less insertion at the 1:80 P/L ratio and a more gradual insertion profile (Fig. 2 *a* and Fig. S2). Aurein 2.2-Δ6, on the other hand, inserted into POPC/POPG bilayers (Fig. 2 *e*) only at higher peptide concentrations, with a threshold P/L ratio between 1:15 and 1:80. The data illustrate that changing L13 to Phe or Val or removing the last three residues of aurein 2.2 did not change the insertion profile of the peptides, as the parent aurein 2.2 also showed a threshold P/L molar ratio between 1:80 and 1:120 (33). Changing L13 to Ala, however, shifted the insertion profile (Fig. S2) more toward that of aurein 2.3, which displayed a threshold P/L ratio between 1:40 and 1:30 (33). Finally, complete removal of L13 by means of the six-residue truncation drastically perturbed the insertion profile of the peptide, making the peptide behave more like aurein 2.3-COOH (33). Overall, this suggests that either removing the long hydrophobic leucine (in the case of aurein 2.2-Δ6) or shortening the side chain (as in L13A) reduced the ability of the peptide to anchor into POPC/POPG membranes. This suggests that residues 11–13 may play an important role in aurein peptide insertion into lipid bilayers.

Lipid headgroup perturbation

^{31}P NMR spectra were recorded for all peptides in 4:1 POPC/POPG (mol/mol) (Figs. 3 and 4) bilayers, as in our previous studies (33). ^{31}P NMR experiments were conducted to determine whether the insertion of the peptides was accompanied by a perturbation of the lipid headgroups, and whether this membrane disruption occurred via a barrel-stave model, carpet model, or toroidal pore model (16,46–49); a micellar aggregate channel model (50,51); or a detergent-like mechanism (52).

In the absence of aurein mutants, the spectra consisted primarily of two single resonances at 30 ppm and 15 ppm (relative ratio of integral of peak at 30 ppm to the one at 15 ppm is 4:1, as determined using DMFIT (53) (not

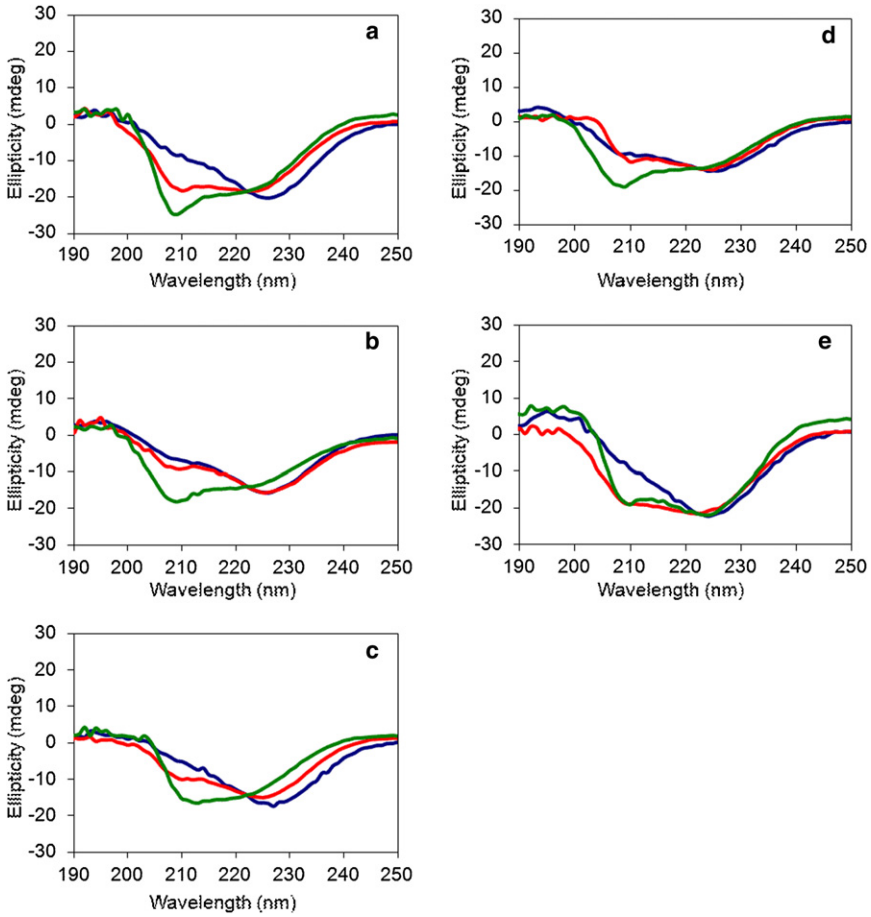

FIGURE 2 Oriented CD spectra of aurein mutants in 1:1 POPC/POPG (mol/mol) bilayers: (*a*) L13A, (*b*) L13F, (*c*) L13V, (*d*) aurein 2.2-Δ3, and (*e*) aurein 2.2-Δ6. The P/L molar ratios are 1:15 (*blue*), 1:80 (*red*), and 1:120 (*green*).

shown)), which indicates that the lipid bilayers were aligned with their normal parallel to the magnetic field (Figs. 3 and 4). We attribute the resonance at 30 ppm as belonging to POPC, and that at 15 ppm as belonging to POPG, given the integrals observed. This would imply that compared to the spectra shown in our previous study (33), the ^{31}P spectra were better resolved. This may be related to an improved alignment achieved by incubating the samples for 8 rather than 7 days, drying the lipids under a stream of N_2 rather than air, and resuspending the lipids in a slightly larger volume of water before depositing them on the slides. However, it is possible that the resonances at 30 and 15 ppm are simply due to different populations of lipids in the samples, with one being more mobile that the other.

In the presence of the aurein mutants, the spectra showed slightly broadened peaks at 30 and 15 ppm, indicating an increased contribution from the unaligned ^{31}P headgroups. In addition, a powder-pattern signal was also observed in the −10 to 30 ppm region, indicative of random headgroup orientations (Figs. 3 and 4). In general, as the concentration of the peptides increased, the contribution of the powder pattern signal became more dominant, as seen in Figs. 3 *d* and 4 *d* (see figure caption for proportion of unaligned signal (54,55)). For the mutants L13A, L13F, and aurein 2.2-Δ3, the line at 30 ppm remained relatively sharp, even at high peptide concentrations (P/L = 1:15), suggesting that a significant proportion of the sample was still reasonably well aligned, i.e., that the lipids formed bilayers. For aurein 2.2-Δ6 (Fig. 4, *right*), however, the degree of lipid headgroup perturbation was more significant, as evidenced by the more intense powder pattern. Finally, for POPC/POPG in the presence of L13V at high concentrations (Fig. 3, *right*), the peak at 30 ppm was broadened substantially and the powder pattern increased significantly at a P/L ratio of 1:15. This suggests that L13V may be more disruptive to the bilayer headgroup alignment than any of the other mutants at high concentrations.

A comparison of the ^{31}P spectra at P/L ratios where the peptides were inserted (based on the OCD findings) suggests that all of the peptides perturbed the bilayers to a similar extent. The underlying powder pattern indicates that the aurein mutants might disorder the bilayer headgroups by the formation of (distorted) toroidal pores (16,46–49).

Antimicrobial activity

Given that all of the five aurein mutants studied here primarily adopt α-helical structures but interact with the

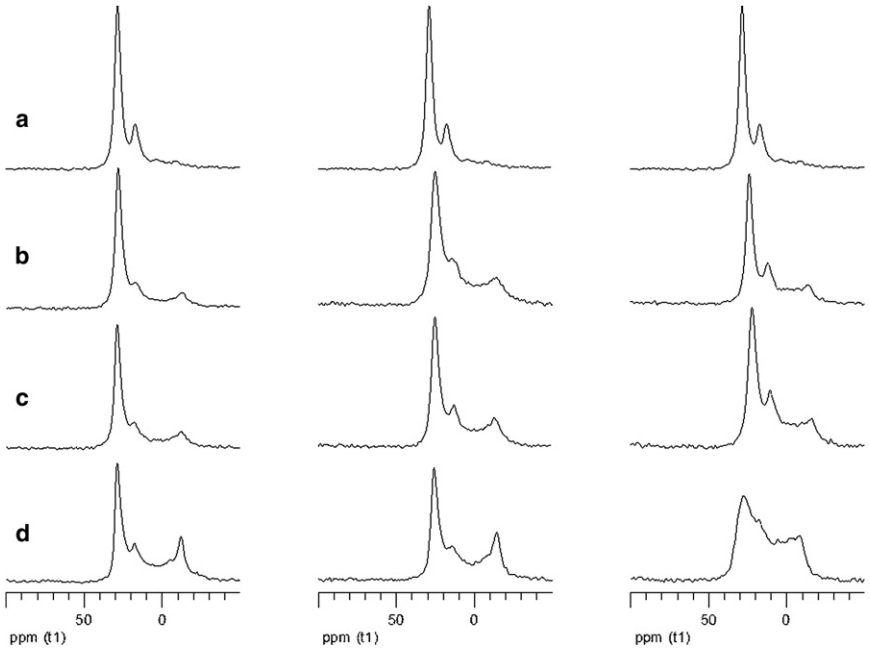

FIGURE 3 Solid-state ^{31}P NMR spectra of mechanically aligned 4:1 POPC/POPG (mol/mol) bilayers containing the three residue 13 aurein mutants: (*a*) POPC/POPG bilayers alone, P/L = (*b*) 1:120, (*c*) 1:80, and (*d*) 1:15 in the presence of L13A (*left panel*), L13F (*center panel*), and L13V (*right panel*). At P/L ratios of 1:15, the proportion of unaligned lipids increases by 34% for L13A, 23% for L13F, and 41% for L13V. These percentages are determined by fitting the spectra in Fig. 3 using two Gaussian/Lorentzian lines and one ^{31}P CSA static line in DMFIT (53) and integrating.

membranes differently, we determined the MICs of all five aurein mutants against two Gram-positive bacteria (*S. aureus* and *S. epidermidis*). The MICs, reported in Table 1, indicate that the L13F, L13V, and L13A mutants have activities very similar to those of the parent peptide, aurein 2.2 (32), under the conditions used here. These mutants had identical MICs of 16 μg/mL against the wild-type *S. aureus* strain C622. Aurein 2.2-Δ3 still showed considerable activity (MIC = 32 μg/mL), whereas aurein 2.2-Δ6 was inactive, with an MIC of 128 μg/mL (4,31). However, the MICs of the L13A, L13F, and L13V mutants against the wild-type *S. epidermidis* strain C621 were slightly different. L13A and L13V showed similar MICs of 8 μg/mL, as did aurein 2.2, whereas L13F had a slightly lower MIC of 16 μg/mL. Likewise, the MICs of the C-terminally truncated mutants were different. Aurein 2.2-Δ3 had an MIC identical to that of the L13A and L13V mutants (8 μg/mL), whereas aurein 2.2-Δ6 again showed no activity, with an MIC of 128 μg/mL. Wells containing polymyxin B, aurein 2.2, culture only, and broth only were used as controls. The MICs observed for polymyxin B and aurein 2.2 are reported in Table 1 and agree with literature findings (32,56). The MICs for all the peptides against the Gram-negative bacteria *Escherichia coli* (MICs $\geq$ 32 μg/mL) support the finding that the aurein peptides are more active against Gram-positive bacteria (57).

Bacterial membrane leakage induced by the aurein mutants

Antimicrobial peptides can kill bacteria through many different mechanisms, one of the most common of which is cytoplasmic membrane depolarization. To observe the effects aurein mutants had on the cytoplasmic membrane of *S. aureus* C622, we carried out membrane depolarization experiments using the membrane-sensitive dye $DiSC_35$. This fluorescent dye is a caged cation that concentrates in the cytoplasmic membrane according to the membrane potential and self-quenches. Destruction of the ionic barrier function of the membrane causes membrane depolarization, release of $DiSC_35$, and a consequent increase (dequenching) of fluorescence. All peptides were compared with the membrane-acting cyclic peptide Gramicidin S. Fig. 5 *a* shows that at 1× MIC, both L13F and aurein 2.2-Δ3 demonstrated greater membrane depolarization than any of the other peptides. L13A and L13V both showed a similar extent of depolarization, whereas aurein 2.2-Δ6 was much less efficient than any other peptide. Fig. 5 *c* illustrates the percentage of membrane depolarization with respect to Gramicidin S at 300 s after peptide addition. The efficiency of membrane depolarization of the five aurein mutants in increasing order was as follows: aurein 2.2-Δ6, L13A/L13V, and L13F/aurein 2.2-Δ3. Increasing the level of aurein peptide added to 5× MIC (Fig. 5 *b*) showed an increased depolarization effect for L13A and aurein 2.2-Δ6, but not for the other mutants (Fig. 5 *d*). This suggests that most mutants, with the exceptions of L13A and aurein 2.2-Δ6, are already at their maximum depolarization efficiency at 1× MIC.

DISCUSSION

Determining which residue is crucial to antimicrobial activity can be a key step in understanding the mechanism

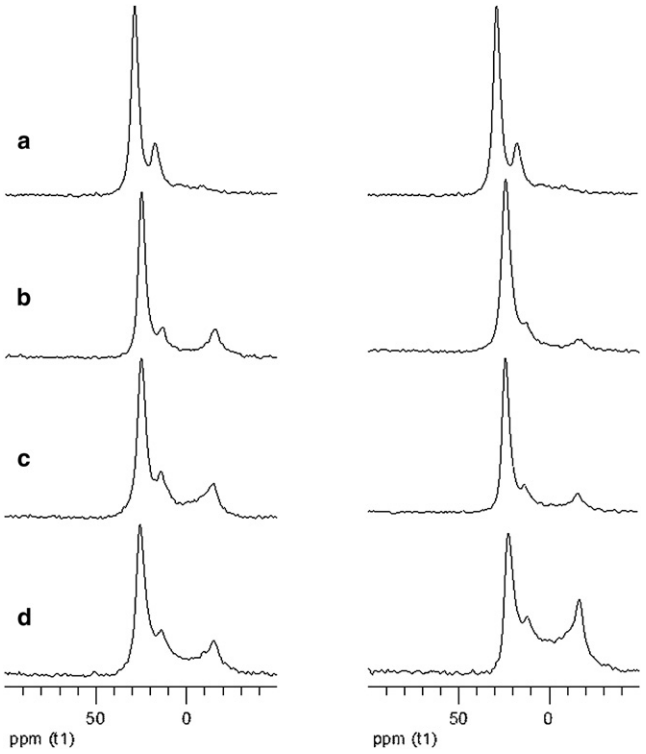

FIGURE 4 Solid-state ^{31}P NMR spectra of mechanically aligned 4:1 POPC/POPG (mol/mol) bilayers containing the two C-terminally truncated aurein mutants: (*a*) POPC/POPG bilayers alone, P/L = (*b*) 1:120, (*c*) 1:80, and (*d*) 1:15 in the presence of aurein 2.2-Δ3 (*left panel*) and aurein 2.2-Δ6 (*right panel*). At P/L ratios of 1:15, the proportion of unaligned lipids increases by 13% for aurein 2.2-Δ3 and 50% for aurein 2.2-Δ6. These percentages are determined by fitting the spectra in Fig. 4 using two Gaussian/Lorentzian lines and one ^{31}P CSA static line in DMFIT (53) and integrating.

of action of a given antimicrobial peptide. In this study we investigated five mutant peptides from aurein 2.2, an antimicrobial peptide from the Australian Southern Bell frog *L. aurea*, to examine how residue-13 substitutions and C-terminal truncations affect structure, membrane interaction, and activity.

Our previous studies demonstrated that aurein 2.2 and aurein 2.3 showed similar antimicrobial activity (32) but perturbed membranes to a different extent (33). Aurein 2.2 and aurein 2.3 differ by only one residue at position 13. Residue specificity at this position may therefore be a key to the difference in the peptide-lipid interactions. When examining a specific residue, one must consider several factors. First, steric hindrance usually plays an important role in peptide/protein activities or folding patterns (58–63). Second, aromatic residues, especially tryptophan, have been shown to promote peptide insertion into the lipid bilayers (34,64). Lastly, hydrophobicity is widely accepted as a key factor in achieving high antimicrobial activity (65,66). Here, we substituted Leu-13 with Ala-13 to test the effect of steric hindrance, Phe-13 to test the importance of aromatic residues, and Val-13 to test the effect of hydrophobic chain length on the structure-function relationship of the aurein 2 family peptides.

Our solution CD results showed that the three aurein mutants L13A, L13F, and L13V adopted α-helical structure in the presence of 1:1 POPC/POPG membranes. Several studies have also demonstrated that mutated antimicrobial peptides adopt similar structures (e.g., human β defensin-1, bacteriocin, and dermcidin (67–70)), similar structures but with varying structural content (e.g., mesentericin Y105 and MSI-78/LL37 analogs (65,71)), or entirely different conformations (e.g., truncated human β defensin-3 (72)). The extent of the change in structure depends on the nature and position of the amino acid that is substituted. We showed here that for relatively conservative substitutions of the aurein peptides, the structures were preserved but the helical contents of the three mutants were different, particularly at low peptide concentrations. This indicates that secondary structure is dependent on the nature of the amino acid at residue 13, in similarity to previous findings from a mesentericin Y105 mutant (71). When we compared the helical content at a P/L ratio of 1:100, we found that L13V was the most helical, followed by aurein 2.2 and aurein 2.3, then L13A, and finally L13F. This trend does not parallel the hydrophobicity trend in the Kyte and Doolittle scale (73), where Ile is more hydrophobic than Val, followed by Leu, Phe, and finally Ala, or in any other available hydrophobicity scale (74,75). This indicates that

TABLE 1 MICs (in μg/mL) of the five aurein mutants, aurein 2.2, and polymyxin B toward *S. aureus* and *S. epidermidis*

Peptide	Sequence	MIC (μg/mL) *S. aureus* (C622)	MIC (μg/mL) *S. epidermidis* (C621)	MIC (μg/mL) *E. coli* (UB1005)
Aurein 2.2-$CONH_2$	GLFDIVKKVVGALGSL	16	8	64
L13A-$CONH_2$	GLFDIVKKVVGAAGSL	16	8	64
L13F-$CONH_2$	GLFDIVKKVVGAFGSL	16	16	64
L13V-$CONH_2$	GLFDIVKKVVGAVGSL	16	8	64
Aurein 2.2-Δ3-$CONH_2$	GLFDIVKKVVGAL	32	8	32
Aurein 2.2-Δ6-$CONH_2$	GLFDIVKKVV	128	128	128
Polymyxin B		50	55	

MICs are given as the most frequently observed value obtained from repeat experiments. Note that all the peptides used in this study are C-terminally amidated.

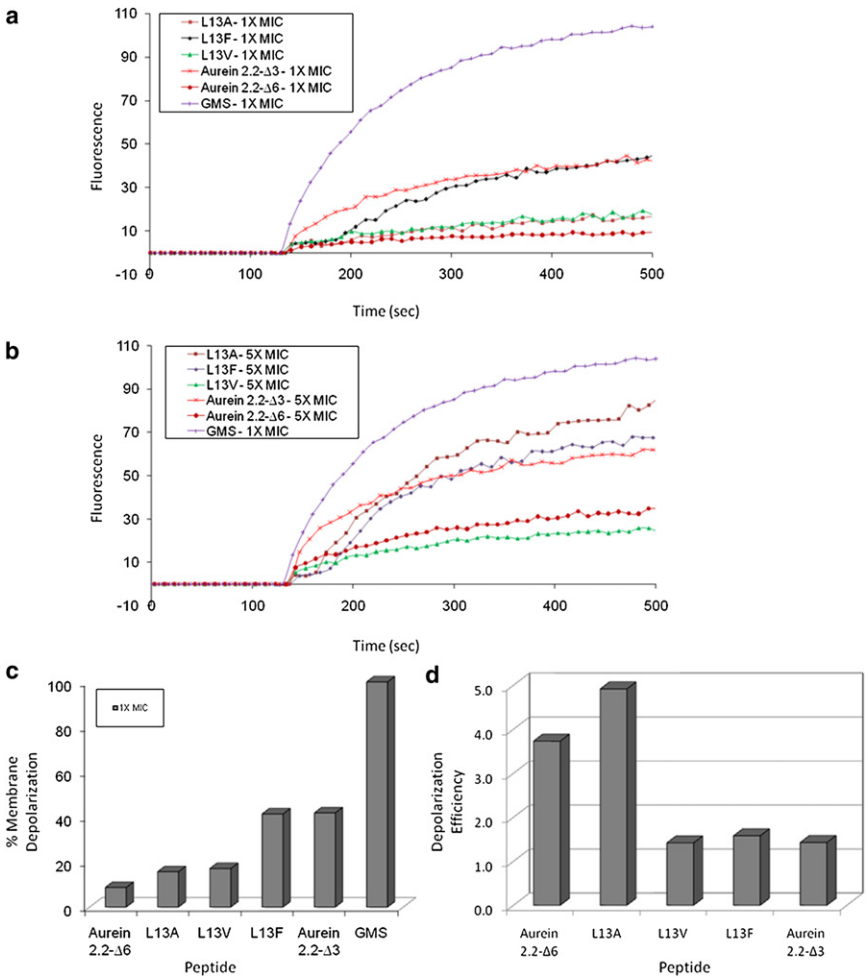

FIGURE 5 Membrane depolarization of *S. aureus* C622 induced by the aurein mutants at 1× and 5× MIC. Gramicidin S (1× MIC) was used as a control. Results are representative of three repeats. (*a* and *b*) $DiSC_35$ release profile of aurein mutants as a function of time at (*a*) 1× and (*b*) 5× MIC. (*c*) Percent membrane depolarization induced by aurein mutants at 300 s after peptide addition with respect to Gramicidin S as the control. (*d*) Membrane depolarization efficiency at 300 s after peptide addition at 5× MIC relative to 1× MIC.

hydrophobicity alone cannot account for structural differences, and that other factors, such as the side chain's bulkiness and its ability to interact with neighboring residues, must play a structural role.

Hydrophobicity alone does not account for how the peptides interacted with POPC/POPG membranes either. The OCD results suggest that L13F, L13V, and aurein 2.2 were the most effective at inserting into POPC/POPG bilayers, with threshold P/L ratios of 1:80–1:120. L13A, on the other hand, was slightly less effective, and aurein 2.3, with an Ile at position 13, was the least effective. Insertion of all the peptides was accompanied by perturbations consistent with toroidal pore formation, as seen in the ^{31}P NMR results here and the results previously reported for aurein 2.2 and 2.3 (33). At low peptide concentrations, the extent of membrane disruption, as indicated by the ^{31}P signals from unoriented headgroups, was similar in the presence of all three mutants. Of interest, however, at high peptide concentrations (1:15 P/L ratio) L13V significantly perturbed the membrane bilayers. Perhaps the high helical content of L13V as seen from the CD data could account for this observation.

The results obtained with the L13A, L13F, and L13V mutants demonstrate that overall it is difficult to clearly correlate subtle changes in sequence with subtle changes in structure and membrane interaction. What the data suggest in broad terms, however, is that the structure and membrane interaction of the aurein peptides correlate reasonably well with the MIC and membrane depolarization. Indeed, aurein 2.2 and L13V, which were the most helical and effective at inserting into and perturbing POPC/POPG bilayers, were effective antimicrobial peptides and depolarized bacterial membranes well. On the other hand, aurein 2.3, which did not readily insert into POPC/POPG bilayers (as seen from the OCD data), also did not depolarize membranes well (33) and was not as good an antimicrobial peptide as aurein 2.2 (32). Of course, comparing data obtained from a bacterial membrane model system with those obtained from bacteria is fraught with danger, but if we are to gain insight into how the aurein peptides function, models are a necessary evil. As presented in a recently submitted manuscript (J. T. J. Cheng, J. D. Hale, J. Kindrachuk, H. Jessen, M. Elliott, R. E. W. Hancock, and S. K. Straus), we explored the choice of bacterial model membranes by

investigating the structure and membrane interaction of aurein 2.2, aurein 2.3, and the mutants studied here in POPE/POPG (1:1) and cardiolipin/POPG (1:1) membranes.

Since the residue-13 substitutions studied here did not significantly influence the structure or peptide-membrane interactions, we also investigated the more dramatic effect of truncating the C-terminus of aurein 2.2. To this end, we examined two C-terminally truncated mutants: one with the last three residues in aurein 2.2 removed (loss of $G_{14}S_{15}L_{16}$) and the other with the last six residues in aurein 2.2 removed (loss of $G_{11}A_{12}\mathbf{L_{13}}G_{14}S_{15}L_{16}$). Both of these deletion mutants retained a predominantly α-helical structure, as seen in the solution CD results (Fig. 1). However, aurein 2.2-Δ6 showed a much lower helical content at all P/L ratios. The extensively truncated aurein 2.2-Δ6 may be too short to form an ordered conformation, as observed for the bioactive gastrin-17 analogs (76) and the $(KIGAKI)_n$ peptide (77). A CD study of magainin-2 also demonstrated that a minimum of 12 residues (with a helical length of 24 ~ 34 Å) is required for antimicrobial activity (78). Both the decreased helical content and the increased random coil content would contribute to the inability of the peptide to perturb lipid membranes to full capacity (77).

Previous studies on cationic antimicrobial peptides have demonstrated that positively charged residues (e.g., Lys and Arg) are important for activity, whereas negatively charged or neutral amino acid (e.g., Asp and Ser) are refractory (79). Aurein 2.2 has two Lys residues located at position 7 and 8, and a Ser at position 15, resulting in a net +2 charge (Table S1). Truncating the first three C-terminal residues removed Ser-15 but did not have an effect on the net charge (Table S1). Our MIC and OCD results showed that this truncation did not have a considerable effect on the antimicrobial activity or the insertion profile of the peptide (aurein 2.2-Δ3). This suggests that the peptide segment $G_{14}S_{15}L_{16}$ is not necessary for antimicrobial activity. Indeed, the activity of aurein 2.2-Δ3 is identical to that of its parent, aurein 2.2. Removal of a larger segment of aurein 2.2, on the other hand, had a significant effect on the antimicrobial activity and insertion profile of the peptide, as seen from our MIC and OCD results. This implies that the peptide segment $G_{11}A_{12}L_{13}$ is crucial for antimicrobial activity and membrane interactions. The GAL segment may be needed as a longer C-terminal hydrophobic segment for better peptide-membrane interactions, or it may provide more effective hydrophobic side-chain packing, as proposed for PMAP-23 (a cathelicidin) (80) and aurein 1.2 (81). It is also possible, however, that aurein 2.2-Δ6 is simply of insufficient peptide length (~15 Å) to span the thicker POPC/POPG bilayers (~39 Å) (82), as was previously observed for the short-chain peptide ampullosporin A (83). This would explain why very high concentrations of aurein 2.2-Δ6 are needed for insertion to occur at all. Once inserted, both aurein 2.2-Δ3 and aurein 2.2-Δ6 perturb the lipids by forming (distorted) toroidal pores.

Overall, the results presented here demonstrate the importance of residue 13 for the structure and function of aurein 2.2. Removal of L13 has a dramatic effect on structure, membrane interaction, toroidal pore formation, MIC, and membrane depolarization. This clearly indicates that the presence of residue 13 is critical for activity. The exact nature of residue 13, however, is less important as long as it is a hydrophobic residue. Indeed, substitution of L13 in aurein 2.2 to Ala, Phe, Val, or Ile (as in aurein 2.3) results in antimicrobial peptides that display similar activities. Presumably, nature has a built-in tolerance to the exact type of amino acid residue at a given position in the cationic antimicrobial peptide, as long as its essential character (e.g., hydrophobicity (84)) is preserved. The fact that the L13 mutants have similar activities but display different extents of membrane depolarization further suggests that there is a tolerance in the exact mechanism that cationic antimicrobial peptides use to kill bacteria (85).

SUPPORTING MATERIAL

Details pertaining to the materials used in this study are available at http://www.biophysj.org/biophysj/supplemental/S0006-3495(10)01165-3.

We thank Fred Rossell of the LMB Spectroscopy hub for his help in maintaining the CD infrastructure, obtained via funding from the Canada Foundation for Innovation.

R.E.W.H. received funding from the Canadian Institutes of Health Research and the Advanced Foods and Materials Network. J.D.H. received a Canadian Commonwealth postdoctoral research fellowship. S.K.S. was supported by the Natural Sciences and Engineering Research Council and the Michael Smith Foundation for Health Research. R.E.W.H. holds a Canada Research Chair.

REFERENCES

1. Devine, D. A., and R. E. W. Hancock. 2002. Cationic peptides: distribution and mechanisms of resistance. *Curr. Pharm. Des.* 8:703–714.
2. Hancock, R. E. W. 2001. Cationic peptides: effectors in innate immunity and novel antimicrobials. *Lancet Infect. Dis.* 1:156–164.
3. Hancock, R. E. W. 2005. Mechanisms of action of newer antibiotics for Gram-positive pathogens. *Lancet Infect. Dis.* 5:209–218.
4. Pukala, T. L., J. H. Bowie, …, M. J. Tyler. 2006. Host-defence peptides from the glandular secretions of amphibians: structure and activity. *Nat. Prod. Rep.* 23:368–393.
5. Rinaldi, A. C. 2002. Antimicrobial peptides from amphibian skin: an expanding scenario. *Curr. Opin. Chem. Biol.* 6:799–804.
6. Zasloff, M. 2002. Antimicrobial peptides of multicellular organisms. *Nature.* 415:389–395.
7. Giovannini, M. G., L. Poulter, …, D. H. Williams. 1987. Biosynthesis and degradation of peptides derived from *Xenopus laevis* prohormones. *Biochem. J.* 243:113–120.
8. Zasloff, M. 1987. Magainins, a class of antimicrobial peptides from *Xenopus* skin: isolation, characterization of two active forms, and partial cDNA sequence of a precursor. *Proc. Natl. Acad. Sci. USA.* 84:5449–5453.
9. Zasloff, M., B. Martin, and H. C. Chen. 1988. Antimicrobial activity of synthetic magainin peptides and several analogues. *Proc. Natl. Acad. Sci. USA.* 85:910–913.

10. Bechinger, B. 2005. Detergent-like properties of magainin antibiotic peptides: a 31P solid-state NMR spectroscopy study. *Biochim. Biophys. Acta.* 1712:101–108.

11. Bechinger, B., M. Zasloff, and S. J. Opella. 1993. Structure and orientation of the antibiotic peptide magainin in membranes by solid-state nuclear magnetic resonance spectroscopy. *Protein Sci.* 2:2077–2084.

12. Duclohier, H., G. Molle, and G. Spach. 1989. Antimicrobial peptide magainin I from *Xenopus* skin forms anion-permeable channels in planar lipid bilayers. *Biophys. J.* 56:1017–1021.

13. Hallock, K. J., D. K. Lee, and A. Ramamoorthy. 2003. MSI-78, an analogue of the magainin antimicrobial peptides, disrupts lipid bilayer structure via positive curvature strain. *Biophys. J.* 84:3052–3060.

14. Jacob, L., and M. Zasloff. 1994. Potential therapeutic applications of magainins and other antimicrobial agents of animal origin. *Ciba Found. Symp.* 186:197–216, discussion 216–223.

15. Ramamoorthy, A., S. Thennarasu, …, L. Maloy. 2006. Solid-state NMR investigation of the membrane-disrupting mechanism of antimicrobial peptides MSI-78 and MSI-594 derived from magainin 2 and melittin. *Biophys. J.* 91:206–216.

16. Yang, L., T. M. Weiss, …, H. W. Huang. 2000. Crystallization of antimicrobial pores in membranes: magainin and protegrin. *Biophys. J.* 79:2002–2009.

17. Ambroggio, E. E., F. Separovic, …, G. D. Fidelio. 2004. Surface behaviour and peptide-lipid interactions of the antibiotic peptides, maculatin and citropin. *Biochim. Biophys. Acta.* 1664:31–37.

18. Ambroggio, E. E., F. Separovic, …, L. A. Bagatolli. 2005. Direct visualization of membrane leakage induced by the antibiotic peptides: maculatin, citropin, and aurein. *Biophys. J.* 89:1874–1881.

19. Balla, M. S., J. H. Bowie, and F. Separovic. 2004. Solid-state NMR study of antimicrobial peptides from Australian frogs in phospholipid membranes. *Eur. Biophys. J.* 33:109–116.

20. Marcotte, I., K. L. Wegener, …, F. Separovic. 2003. Interaction of antimicrobial peptides from Australian amphibians with lipid membranes. *Chem. Phys. Lipids.* 122:107–120.

21. Niidome, T., K. Kobayashi, …, H. Aoyagi. 2004. Structure-activity relationship of an antibacterial peptide, maculatin 1.1, from the skin glands of the tree frog, *Litoria genimaculata*. *J. Pept. Sci.* 10:414–422.

22. Boland, M. P., and F. Separovic. 2006. Membrane interactions of antimicrobial peptides from Australian tree frogs. *Biochim. Biophys. Acta.* 1758:1178–1183.

23. Chen, T., L. Li, …, C. Shaw. 2006. Amphibian skin peptides and their corresponding cDNAs from single lyophilized secretion samples: identification of novel brevinins from three species of Chinese frogs. *Peptides.* 27:42–48.

24. Conlon, J. M., N. Al-Ghaferi, …, H. Vaudry. 2006. Antimicrobial peptides from diverse families isolated from the skin of the Asian frog, *Rana grahami*. *Peptides.* 27:2111–2117.

25. Kumari, V. K., and R. Nagaraj. 2001. Structure-function studies on the amphibian peptide brevinin 1E: translocating the cationic segment from the C-terminal end to a central position favors selective antibacterial activity. *J. Pept. Res.* 58:433–441.

26. Morikawa, N., K. Hagiwara, and T. Nakajima. 1992. Brevinin-1 and -2, unique antimicrobial peptides from the skin of the frog, *Rana brevipoda porsa*. *Biochem. Biophys. Res. Commun.* 189:184–190.

27. Simmaco, M., G. Mignogna, …, F. Bossa. 1993. Novel antimicrobial peptides from skin secretion of the European frog *Rana esculenta*. *FEBS Lett.* 324:159–161.

28. Won, H. S., S. S. Kim, …, B. J. Lee. 2004. Structure-activity relationships of antimicrobial peptides from the skin of *Rana esculenta* inhabiting in Korea. *Mol. Cells.* 17:469–476.

29. Apponyi, M. A., T. L. Pukala, …, L. E. Llewellyn. 2004. Host-defence peptides of Australian anurans: structure, mechanism of action and evolutionary significance. *Peptides.* 25:1035–1054.

30. Rozek, T., J. H. Bowie, …, M. J. Tyler. 2000. The antibiotic and anticancer active aurein peptides from the Australian bell frogs *Litoria aurea* and *Litoria raniformis*. Part 2. Sequence determination using electrospray mass spectrometry. *Rapid Commun. Mass Spectrom.* 14:2002–2011.

31. Rozek, T., K. L. Wegener, …, M. J. Tyler. 2000. The antibiotic and anticancer active aurein peptides from the Australian bell frogs *Litoria aurea* and *Litoria raniformis* the solution structure of aurein 1.2. *Eur. J. Biochem.* 267:5330–5341.

32. Pan, Y. L., J. T. J. Cheng, …, S. K. Straus. 2007. Characterization of the structure and membrane interaction of the antimicrobial peptides aurein 2.2 and 2.3 from Australian Southern Bell frogs. *Biophys. J.* 92:2854–2864.

33. Cheng, J. T., J. D. Hale, …, S. K. Straus. 2009. Effect of membrane composition on antimicrobial peptides aurein 2.2 and 2.3 from Australian Southern Bell frogs. *Biophys. J.* 96:552–565.

34. Dathe, M., H. Nikolenko, …, M. Bienert. 2004. Cyclization increases the antimicrobial activity and selectivity of arginine- and tryptophan-containing hexapeptides. *Biochemistry.* 43:9140–9150.

35. Dathe, M., H. Nikolenko, …, M. Bienert. 2001. Optimization of the antimicrobial activity of magainin peptides by modification of charge. *FEBS Lett.* 501:146–150.

36. Hilpert, K., M. R. Elliott, …, R. E. Hancock. 2006. Sequence requirements and an optimization strategy for short antimicrobial peptides. *Chem. Biol.* 13:1101–1107.

37. Lewis, R. N., F. Liu, …, R. N. McElhaney. 2007. Studies of the minimum hydrophobicity of α-helical peptides required to maintain a stable transmembrane association with phospholipid bilayer membranes. *Biochemistry.* 46:1042–1054.

38. Wieprecht, T., M. Dathe, …, M. Bienert. 1997. Modulation of membrane activity of amphipathic, antibacterial peptides by slight modifications of the hydrophobic moment. *FEBS Lett.* 417:135–140.

39. Wu, M., and R. E. Hancock. 1999. Interaction of the cyclic antimicrobial cationic peptide bactenecin with the outer and cytoplasmic membrane. *J. Biol. Chem.* 274:29–35.

40. Reference deleted in proof.

41. Johnson, W. C. 1999. Analyzing protein circular dichroism spectra for accurate secondary structures. *Proteins.* 35:307–312.

42. Provencher, S. W., and J. Glöckner. 1981. Estimation of globular protein secondary structure from circular dichroism. *Biochemistry.* 20:33–37.

43. Sreerama, N., S. Y. Venyaminov, and R. W. Woody. 1999. Estimation of the number of α-helical and β-strand segments in proteins using circular dichroism spectroscopy. *Protein Sci.* 8:370–380.

44. Sreerama, N., and R. W. Woody. 1994. Protein secondary structure from circular dichroism spectroscopy. Combining variable selection principle and cluster analysis with neural network, ridge regression and self-consistent methods. *J. Mol. Biol.* 242:497–507.

45. Sreerama, N., and R. W. Woody. 1993. A self-consistent method for the analysis of protein secondary structure from circular dichroism. *Anal. Biochem.* 209:32–44.

46. Shai, Y. 1999. Mechanism of the binding, insertion and destabilization of phospholipid bilayer membranes by α-helical antimicrobial and cell non-selective membrane-lytic peptides. *Biochim. Biophys. Acta.* 1462:55–70.

47. Papo, N., and Y. Shai. 2005. Host defense peptides as new weapons in cancer treatment. *Cell. Mol. Life Sci.* 62:784–790.

48. Matsuzaki, K. 1999. Why and how are peptide-lipid interactions utilized for self-defense? Magainins and tachyplesins as archetypes. *Biochim. Biophys. Acta.* 1462:1–10.

49. Huang, H. W. 2000. Action of antimicrobial peptides: two-state model. *Biochemistry.* 39:8347–8352.

50. Wu, M., E. Maier, …, R. E. Hancock. 1999. Mechanism of interaction of different classes of cationic antimicrobial peptides with planar bilayers and with the cytoplasmic membrane of Escherichia coli. *Biochemistry.* 38:7235–7242.

51. Hancock, R. E. W., and D. S. Chapple. 1999. Peptide antibiotics. *Antimicrob. Agents Chemother.* 43:1317–1323.

52. Bechinger, B., and K. Lohner. 2006. Detergent-like actions of linear amphipathic cationic antimicrobial peptides. *Biochim. Biophys. Acta.* 1758:1529–1539.

53. Massiot, D., F. Fayon, …, G. Hoatson. 2002. Modelling one- and two-dimensional solid-state NMR spectra. *Magn. Reson. Chem.* 40:70–76.

54. Ouellet, M., J. D. Doucet, …, M. Auger. 2007. Membrane topology of a 14-mer model amphipathic peptide: a solid-state NMR spectroscopy study. *Biochemistry.* 46:6597–6606.

55. Wi, S., and C. Kim. 2008. Pore structure, thinning effect, and lateral diffusive dynamics of oriented lipid membranes interacting with antimicrobial peptide protegrin-1: 31P and 2H solid-state NMR study. *J. Phys. Chem. B.* 112:11402–11414.

56. Falla, T. J., and R. E. Hancock. 1997. Improved activity of a synthetic indolicidin analog. *Antimicrob. Agents Chemother.* 41:771–775.

57. Bowie, J. H., K. L. Wegener, …, J. C. Wallace. 1999. Host defence antibacterial peptides from skin secretions of Australian amphibians. The relationship between structure and activity. *Protein Pept. Lett.* 6: 259–269.

58. Fowler, S. M., R. J. Riley, …, C. R. Wolf. 2000. Amino acid 305 determines catalytic center accessibility in CYP3A4. *Biochemistry.* 39:4406–4414.

59. Holst, B., S. Zoffmann, …, T. W. Schwartz. 1998. Steric hindrance mutagenesis versus alanine scan in mapping of ligand binding sites in the tachykinin NK1 receptor. *Mol. Pharmacol.* 53:166–175.

60. Marana, S. R., W. R. Terra, and C. Ferreira. 2002. The role of amino-acid residues Q39 and E451 in the determination of substrate specificity of the *Spodoptera frugiperda* β-glycosidase. *Eur. J. Biochem.* 269:3705–3714.

61. Runkel, L., C. De Dios, …, P. S. Hochman. 2001. Mapping of IFN-β epitopes important for receptor binding and biologic activation: comparison of results achieved using antibody-based methods and alanine substitution mutagenesis. *J. Interferon Cytokine Res.* 21: 931–941.

62. Sekine, O., T. Sugo, …, M. Matsudai. 2002. Substitution of Gly-548 to Ala in the substrate binding pocket of prothrombin Perijá leads to the loss of thrombin proteolytic activity. *Thromb. Haemost.* 87:282–287.

63. Wei, Z., and S. J. Swiedler. 1999. Functional analysis of conserved cysteines in heparan sulfate N-deacetylase-N-sulfotransferases. *J. Biol. Chem.* 274:1966–1970.

64. Lazaridis, T. 2005. Implicit solvent simulations of peptide interactions with anionic lipid membranes. *Proteins.* 58:518–527.

65. Radzishevsky, I. S., S. Rotem, …, A. Mor. 2005. Effects of acyl versus aminoacyl conjugation on the properties of antimicrobial peptides. *Antimicrob. Agents Chemother.* 49:2412–2420.

66. Shafer, W. M., S. Katzif, …, J. Pohl. 2002. Tailoring an antibacterial peptide of human lysosomal cathepsin G to enhance its broad-spectrum action against antibiotic-resistant bacterial pathogens. *Curr. Pharm. Des.* 8:695–702.

67. Chandrababu, K. B., B. Ho, and D. Yang. 2009. Structure, dynamics, and activity of an all-cysteine mutated human β defensin-3 peptide analogue. *Biochemistry.* 48:6052–6061.

68. Pazgier, M., A. Prahl, …, J. Lubkowski. 2007. Studies of the biological properties of human β-defensin 1. *J. Biol. Chem.* 282:1819–1829.

69. Sánchez-Hidalgo, M., M. Martínez-Bueno, …, M. Maqueda. 2008. Effect of replacing glutamic residues upon the biological activity and stability of the circular enterocin AS-48. *J. Antimicrob. Chemother.* 61:1256–1265.

70. Steffen, H., S. Rieg, …, B. Schittek. 2006. Naturally processed dermcidin-derived peptides do not permeabilize bacterial membranes and kill microorganisms irrespective of their charge. *Antimicrob. Agents Chemother.* 50:2608–2620.

71. Morisset, D., J. M. Berjeaud, …, J. Frère. 2004. Mutational analysis of mesentericin y105, an anti-Listeria bacteriocin, for determination of impact on bactericidal activity, in vitro secondary structure, and membrane interaction. *Appl. Environ. Microbiol.* 70:4672–4680.

72. Antcheva, N., F. Morgera, …, A. Tossi. 2009. Artificial β-defensin based on a minimal defensin template. *Biochem. J.* 421:435–447.

73. Kyte, J., and R. F. Doolittle. 1982. A simple method for displaying the hydropathic character of a protein. *J. Mol. Biol.* 157:105–132.

74. Miyazawa, S., and R. L. Jernigan. 1985. Estimation of effective interresidue contact energies from protein crystal-structures—quasi-chemical approximation. *Macromolecules.* 18:534–552.

75. Abraham, D. J., and A. J. Leo. 1987. Extension of the fragment method to calculate amino acid zwitterion and side chain partition coefficients. *Proteins.* 2:130–152.

76. Copps, J., R. F. Murphy, and S. Lovas. 2009. The structure of bioactive analogs of the N-terminal region of gastrin-17. *Peptides.* 30:2250–2262.

77. Meier, M., and J. Seelig. 2008. Length dependence of the coil $<\!\!-\!\!>$ β-sheet transition in a membrane environment. *J. Am. Chem. Soc.* 130:1017–1024.

78. Patch, J. A., and A. E. Barron. 2003. Helical peptoid mimics of magainin-2 amide. *J. Am. Chem. Soc.* 125:12092–12093.

79. Wegener, K. L., P. A. Wabnitz, …, M. J. Tyler. 1999. Host defence peptides from the skin glands of the Australian blue mountains treefrog *Litoria citropa*. Solution structure of the antibacterial peptide citropin 1.1. *Eur. J. Biochem.* 265:627–637.

80. Yang, S. T., J. H. Jeon, …, J. I. Kim. 2006. Possible role of a PXXP central hinge in the antibacterial activity and membrane interaction of PMAP-23, a member of cathelicidin family. *Biochemistry.* 45:1775–1784.

81. Wang, G. 2010. Structure, dynamics and mapping of membrane-binding residues of micelle-bound antimicrobial peptides by natural abundance (13)C NMR spectroscopy. *Biochim. Biophys. Acta.* 1798:114–121.

82. Leidy, C., L. Linderoth, …, G. H. Peters. 2006. Domain-induced activation of human phospholipase A2 type IIA: local versus global lipid composition. *Biophys. J.* 90:3165–3175.

83. Salnikov, E. S., H. Friedrich, …, B. Bechinger. 2009. Structure and alignment of the membrane-associated peptaibols ampullosporin A and alamethicin by oriented 15N and 31P solid-state NMR spectroscopy. *Biophys. J.* 96:86–100.

84. Jiang, Z., B. J. Kullberg, …, R. S. Hodges. 2008. Effects of hydrophobicity on the antifungal activity of α-helical antimicrobial peptides. *Chem. Biol. Drug Des.* 72:483–495.

85. Hale, J. D., and R. E. Hancock. 2007. Alternative mechanisms of action of cationic antimicrobial peptides on bacteria. *Expert Rev. Anti Infect. Ther.* 5:951–959.